Available online at www.sciencedirect.com
ScienceDirect
Journal of Sound and Vibration 308 (2007) 709–720
JOURNAL OF SOUND AND VIBRATION
www.elsevier.com/locate/jsvi

# Low-frequency vibroisolation mounting of power plants for new-generation airplanes with engines of extra-high bypass ratio

Viatcheslav S. Baklanov

*Vibroacoustics and APU Department, Central Design Bureau, Power Plant Division, Academician Tupolev Emb., 17, "Tupolev", 105005 Moscow, Russia*

Accepted 12 April 2007
The peer review of this article was organized by the Guest Editor
Available online 23 July 2007

**Abstract**

Compliance of aircraft with new noise standards defines the tendency to switch to extra-high bypass-ratio engines.

Substantial noise redistribution has occurred in the aircraft of the new generation. While jet noise has been reduced dramatically, the engine still remains to be the basic source of noise, which is a fan noise. In the forward hemisphere, besides the discrete components at fan blade frequency, long row of discrete components has been observed around the principal blade frequencies as a result of shockwave influence. This phenomenon is called "buzz-saw noise".

Fan shaft frequency reduction is one of the necessary measures for shockwaves control. Due to the decrease of frequency, the vibration spectrum shifts towards the low-frequency range. Such components will determine the dynamical impact spectrum of power plant, transmitted through mounting to airframe construction. An airframe typically possesses dozens of oscillation the modes in the low-frequency spectrum part. Interaction of some of them with the influence of the power plant may generate discrete low-frequency high-level noise components in the cabin.

We have designed new low-frequency attachments containing built-in elastic elements with nonlinear characteristics and with a quasi-zero stiffness zone at proof load by the cruise mode.


## 1. Introduction

The investigations carried out within Quiet Technology Demonstrator have yielded the presence of so-called buzz-saw noise, discovered in the front cabin of B-777-200 ER equipped by Trent 800 [1].

Buzz-saw noise in the cabin is a special feature of extra-high bypass-ratio engine fan emission. It manifests itself in the rise of a long row of discrete spectral components around the principal blade frequencies (first and second harmonics) in the forward hemisphere (Fig. 1) [1]. Fan diameter increasing in high-bypass-ratio engines, fan blades start rotating at ultrasonic speed, thus generating shockwaves. The shockwave interaction with fan generates a polyharmonical field with discrete components.

Buzz-saw noise is one part (high-frequency region) of the spectrum of noise expected in the pressurized cabin of new-generation engines with extra-high bypass ratio. The other part of the spectrum is the

*E-mail address:* baklanov@tupolev.ru

0022-460X/$ - see front matter © 2007 Elsevier Ltd. All rights reserved.
doi:10.1016/j.jsv.2007.04.042

**Nomenclature**

$\mathbf{C}_{AM}$ square matrix of the airframe structure dynamic compliances at attachment points
$C^i_{AM}(f)$ airframe dynamic compliances at the $i$th point of coupling, cm/kg
$\mathbf{C}_{EM}$ square matrix of the engine casing structure dynamic compliances at attachment points
$C^i_{EM}(f)$ engine casing dynamic compliances at the $i$th point of coupling, cm/kg
$\mathbf{C}_{ES}$ square matrix of transition compliances of the engine structure from points of exciting forces application within the engine components to attachment points
$C^{ki}_{ES}(f)$ transfer engine structure dynamic compliance, cm/kg
$C^i_{is}$ vibroisolator compliance
$f$ frequency
$\mathbf{F}_E$ column matrix of exciting forces within the engine components
$F^k_E(f)$ engine exciting force, kg
$F^i_{sh}(f)$ exciting force value of the airframe when acoustic conductance function is determined, kg
$H^{in}_A(f)$ transfer function characterizing acoustic conductance of the airframe structure from the engine vibration exciting points (attachment points) to noise measurement locations
$\mathrm{Im}\, C$ imaginary part of $C$
$L^{in}_{H_A}(f)$ function of the airframe structure acoustic conductance up to point $n$ if effect at the $i$th point has the force assumed in the course of the experiment in dB
$P^n(f)$ sound-pressure level at some point $n$ of the pressurized cabin, cm/kg$^2$
$\mathbf{R}_A$ column matrix of reactions at attachment points that characterizes the engine dynamic effect
$\mathbf{R}_E$ column matrix of reactions at attachment points that characterizes the engine dynamic effect
$R^i_E(f)$ level of the engine dynamic effect upon the airframe structure at the $i$th point of coupling
$\mathrm{Re}\, C$ real part of $C$
$V^i_E(f)$ the engine casing vibration level near the $i$th point of coupling, cm/s
$\mathbf{X}_A$ column matrix of airplane displacements
$\mathbf{X}_E$ column matrix of engine displacements
$Z$ number of fan blades

low-frequency region, which includes rotor frequencies of the three shafts and duct low-frequency components have not been shown in Fig. 1.

The vibration spectrum of turbofan engines, especially of those with high bypass ratio, substantially extends due to the possible use of low speed of the fan rotor, 2–3 shaft schemes and low-frequency terms of perturbation action of the engine gas-air flow duct.

Vibration contribution to the acoustic properties of the pressurized cabin has been determined during the investigations of the vibroisolating engine mount, which was designed taking into account the real dynamic characteristics (engine case and airframe dynamic compliance) [2].

In Fig. 2 the experimental vibration spectra for front (b) and back (c) mounting and noise spectrum in cabin (a) are represented. A series of polyharmonic discrete components have been observed in the spectrum of engine case vibrations especially for the front mount location. These components are grouped around the main blade frequencies (the first and the second harmonics), the distance between the components and blade frequency being equal to the shaft rotation frequency. This yields a formula for the position of the corresponding peak in spectrum:

$$f = \sum_{m=1,\ldots,n}^{i} m f_s(z \pm i). \tag{1}$$

Here $f$ is the frequency of discrete components, $f_s$ is the fan shaft rotation frequency, $z$ is the number of fan blades, $m$ is the number of harmonics at blade frequency, and $i = 0, 1, 2 \ldots k$.

All these components of the vibration spectrum, as well as the discrete components of vibroactive devices, installed in the engine (e.g., plunger pump), or the spectral components of new devices (e.g., chevron nozzles,

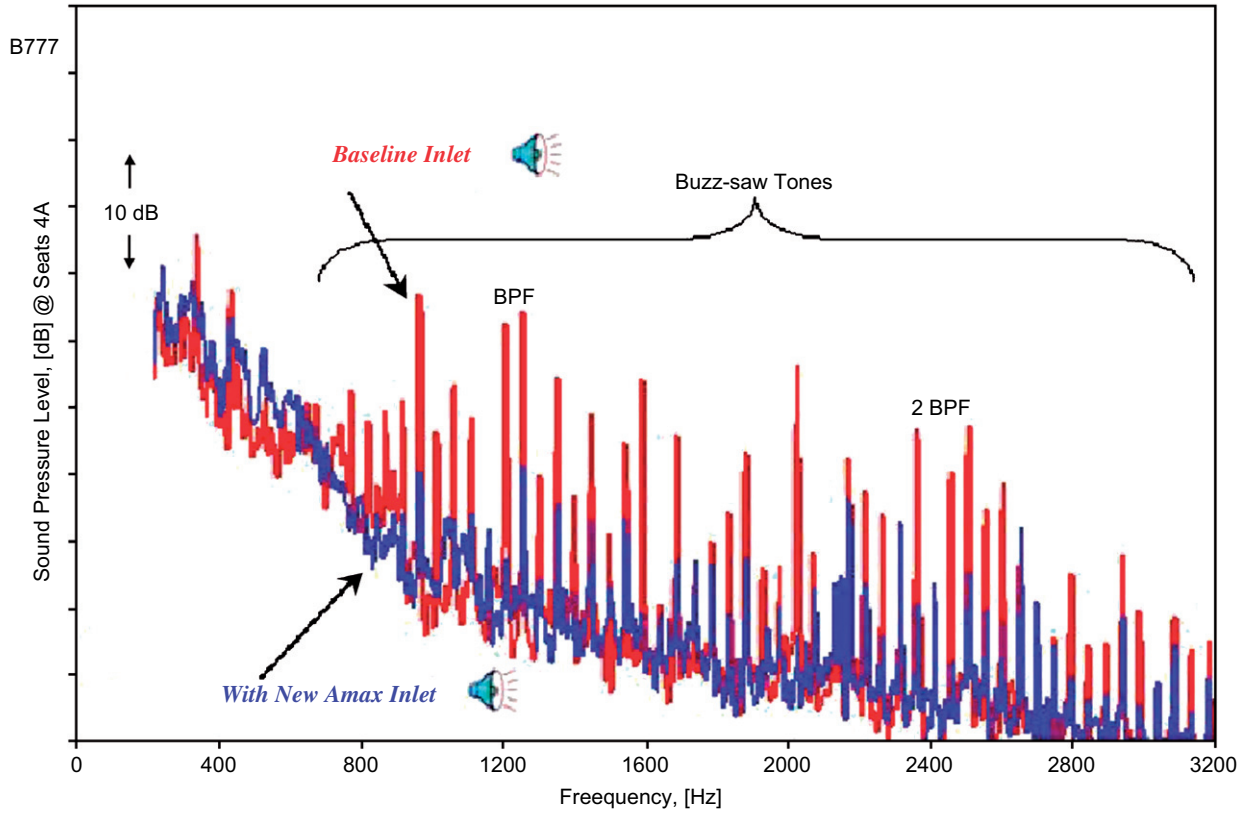


Fig. 1. Buzz-saw noise decrease in a B-777 cabin (new inlet).

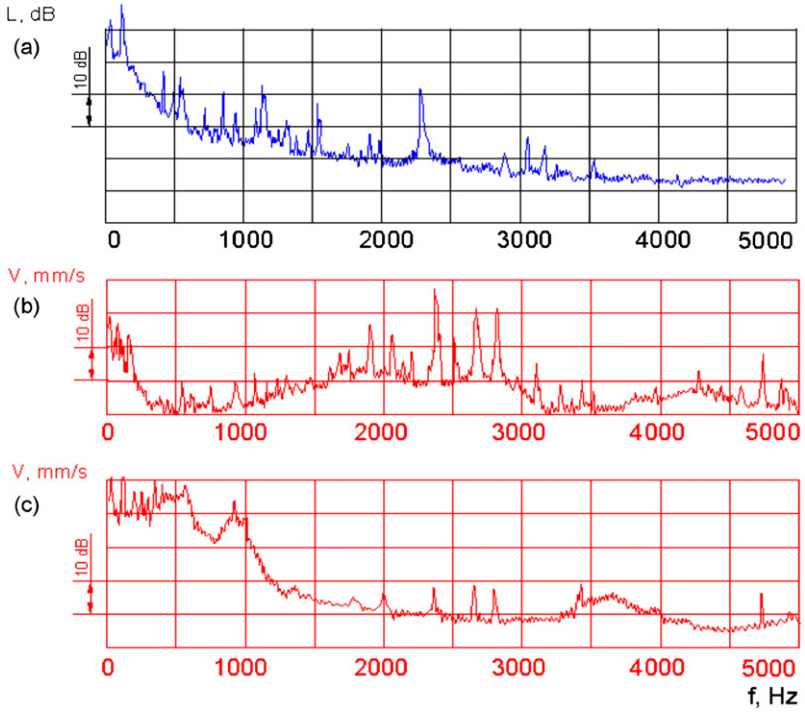


Fig. 2. Noise and vibration spectrums (various locations of the sensor). (a) Noise spectrum in the pressurized cabin (engine-mount zone); (b) vibrations spectrum of the engine case (front mount); and (c) vibrations spectrum of the engine case (after ? mount).

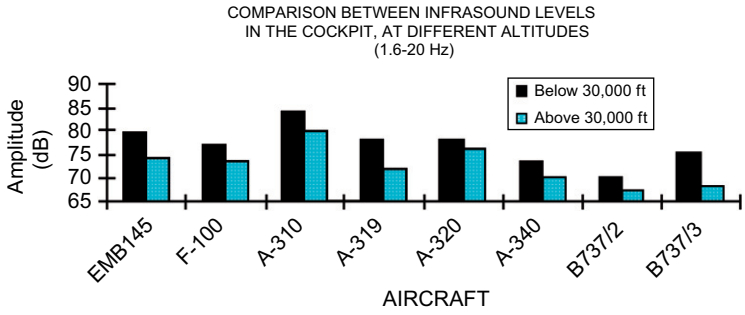


Fig. 3. Level of infrasound components in the crew cabin.

introduced into the stream and supplementing the vibration spectrum of engine case) will be a source of structure-borne noise, transferred via mounting points onto the airframe and re-emitted into the pressurized cabin.

A sparse series of high-frequency noise components, in comparison with Fig. 1, is observed in the pressurized cabin noise (Fig. 2), but an impressive series of low-frequency components is also reported in the spectrum (corresponding to fan shaft harmonics and the plunger pump harmonic).

Investigations of the Portuguese Medical Center point out the increased level of infrasound components in crew cabin with regard to passenger cabin in modern airplanes (Fig. 3) [3].

These components arise both due to the exciting impact of incoming flow and due to the effect of the power plant–airframe interaction mentioned above. These data cause anxiety due to possible increases of these components when switching to high-bypass-ratio engines.

Unfortunately, the problems of the properties of structure-borne noise inside the pressurized cabin being changed by introducing high-bypass-ratio engines are still beyond the scope of the general discussion.

We believe that solving problems of structure noise for high-bypass-ratio engines require serious refining of "engine-mount-airframe" system models.

## 2. Calculation model

In the paper, the calculated model that takes into account real dynamic characteristics of modern designs, which are characterized by a matrix of dynamic compliance of the engine body at the attachment points and the answer attachment points on an airframe and also by tensor of transfer functions from attachment points with various cabin elements, are discussed.

Examples of successful application of such characteristics are known. One of the first times when such research was performed in current aviation (1967) was an investigation of a DC-9 aircraft in the course of activities on eliminating reasons for increase of noise level in the cabin of the aircraft. But this analysis was confined to the airframe and the engine body impedance determination in one attachment point [4].

For the first time, a broad investigation of the set of dynamic compliances at the tail end of the airframe (the place of central engine location) and at the pods (the place of side engines location) and dynamical compliances of engine's body at the attachment points was carried out (1973) at the first specimens of the TU-154 aircraft with NK-8-2U engines.

The new procedure of estimation of engine dynamic impact on the airframe and of structural noise, created by engine vibration, was suggested on the basis of studying the airframe and engine body dynamic characteristics and the dynamic loading of engine struts.

This procedure was realized during the Program by researching dynamic compliances of the TU-154M airframe and the engine D-30KU body, and also by testing the transfer function of vibroacoustic conductivities of the airframe design between impact points (engine-mounting units) and the noise and vibration-level check points (crew and passenger cabins) [5].

An analogy for this procedure was used in USA for a light airplane (Cessna 172) transmission model that includes airframe dynamic characteristics at the attachment points and the acoustic response of

selected cabin interior points and determined by impedance testing, but the engine was represented as a rigid body [6].

The multi-connected dynamic model of the system "Engine-mount-airframe" can be studied by dividing it into independent sub-systems (Fig. 4), reaction forces being applied in the separation points. Then the differential equations for the displacements of separation points are written down, where the generalized dynamic characteristics (for example, dynamic compliance) are used as factors of proportionality between dynamic displacement and forces.

Writing matrix equations for displacements in separation points for each system, one can obtain:

$$\begin{aligned} \mathbf{X}_E &= \mathbf{C}_{ES}\mathbf{F}_E + \mathbf{C}_{EM}\mathbf{R}_E, \\ \mathbf{X}_A &= \mathbf{C}_{AM}\mathbf{R}_A. \end{aligned} \tag{2}$$

Taking into account that $\mathbf{X}_E = \mathbf{X}_A$ and reactions in these (separation) points are $\mathbf{R}_E = -\mathbf{R}_A$, an expression for estimation of level of engine's dynamical impact on airframe can be obtained:

$$\mathbf{R}_E = (\mathbf{C}_{EM} + \mathbf{C}_{AM})^{-1}\mathbf{C}_{ES}\mathbf{F}_{ES}. \tag{3}$$

Using the set of real dynamic compliances of the engines and airframes, defined by the experimental way, the limits of coupled vibrations of the "engine-attachment-airframe" system and the possibility of presentation of the system in the form of independent one-dimensional vectors (vibroconduits) were investigated.

In case of dynamic independence of engine-mounting attachments, the equation for dynamic forces, acting from the side of the engine at $i$-coupling point, can be reduced to the following form:

$$R_E^i(f) = \left[C_{EM}^i(f) + C_{AM}^i(f)\right]^{-1} \sum_{k=1}^{m} C_{ES}^{ki}(f) F_E^k(f), \tag{4}$$

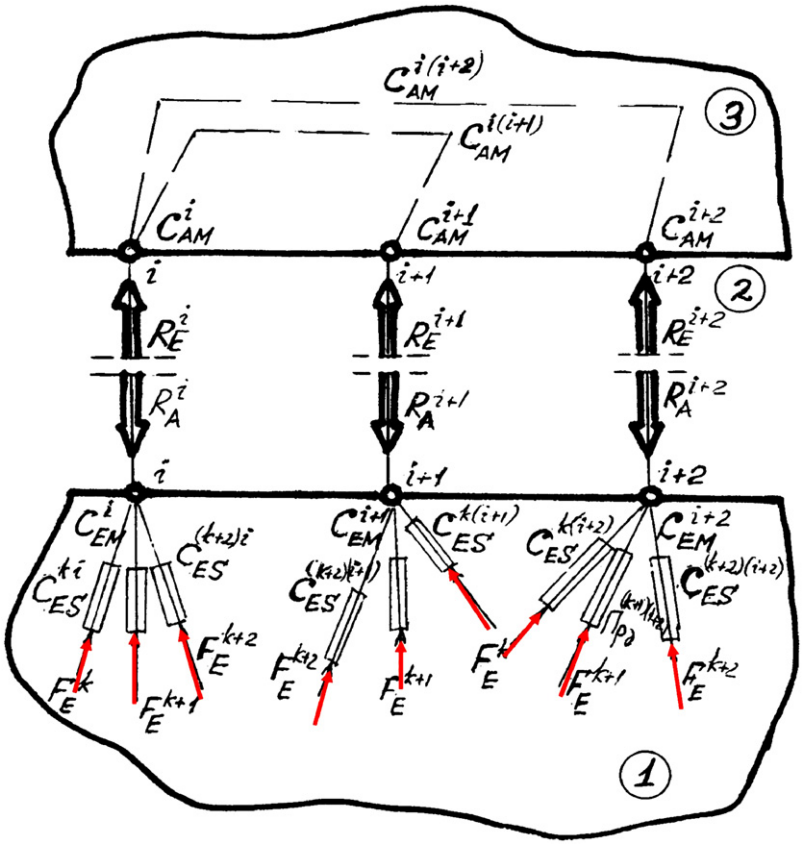


Fig. 4. Multi-coupled dynamic model for the "engine-mount-airframe" system.

where the expression $\sum_{k=1}^{m} C_{ES}^{ki}(f)F_E^k(f)$ characterizes engine vibration activity and is the engine excursion at attachment points (as a rule, where the standard vibration pickups are installed). The obtained expression allows one to estimate an expecting dynamical impact level from basic sources (residual disbalance of engine's rotors) and from other vibroactive elements installed on the engine (hydropumps, gearbox, perturbations in engine's gas-air flow duct).

Considering each $i$th coupling of $m$ engine support couplings with the airframe structure as a separate source of exciting, we can determine sound-pressure level $p^n$, which is generated at some point $n$ of the pressurized cabin as a sum of sound-pressure values excited by each said source:

$$p^n(f) = \sum_{i=1}^{m} H_A^{in}(f)R_E^i(f). \tag{5}$$

After dB-noise evaluation can be written as

$$L^{ni}(f) = L_{H_A}^{in}(f) + 20\,lg(C_{ES}^i(f) + C_{AS}^i(f))^{-1}\frac{V_E^i(f)}{2\pi f F_{sh}^i(f)}. \tag{6}$$

Power combining the separate sources of all engines (in view of co-physic effect in all engine attachment points), The total noise level of Power Plant vibration exciting can be obtained [7].

Reduction of the level of engine dynamic effect on the aircraft can be provided, for example, by building in vibroisolation units into the engine attachments, and then effectiveness ($\Delta L^i$) of application of such units in case of dynamic independence of separate vibroconduits is defined for the $i$-attachment from the following expression:

$$\Delta L^i(f) = 20\,lg\frac{1}{\eta_i} = 20\,lg\left|\frac{C_{EM}^i(f) + C_{AM}^i(f) + C_{is}^i}{C_{EM}^i(f) + C_{AM}^i(f)}\right|, \tag{7}$$

where

$$\eta_i = \frac{R^i(f)\text{ in case of vibroisolating mount}}{R^i(f)\text{ in case of rigid attachment}}.$$

From the latter of the expressions, we can define vibroisolator compliance to ensure the required level of reduction ($\eta_0$) of the forces transmitted to the aircraft:

$$C_{is}^i \geqslant \frac{1}{\eta_0}\sqrt{\left(\mathrm{Re}C_{EM}^i + \mathrm{Re}C_{AM}^i\right)^2 + \left(\mathrm{Im}C_{EM}^i + \mathrm{Im}C_{AM}^i\right)^2\left(1-\eta_0^2\right)} - \left(\mathrm{Re}C_{EM}^i + \mathrm{Re}C_{AM}^i\right), \tag{8}$$

where $\mathrm{Re}C_{EM}^i$, $\mathrm{Re}C_{AM}^i$, $\mathrm{Im}C_{EM}^i$, $\mathrm{Im}C_{AM}^i$ are the real and imaginary components of dynamic compliances for the engine and aircraft, respectively, in the locations of the $i$th attachment.

Different natures of structural dynamic behavior (the inertial one and the elastic one) convince us of the necessity to know the real dynamic characteristics of an engine and aircraft at mounting points so that effective vibroisolating mountings of the engine can be developed [8].

## 3. Experimental data analysis

Several analytical models are considered together nowadays to predict the acoustic properties of the cabin. Although design models of the airframe, the pylon and the cabin take into account some thousands of freedom degrees, the engine is still considered to be a rigid body, taking into account-only its mass and moments of inertia.

This is due to an old tradition of successful flutter calculations, as the rigid-body engine model is still true in that range (low-frequency range, below 15 Hz).

The dynamic characteristics enabled us to make the dynamic model for an aviation gas-turbine engine more precise, especially in the rotor frequency range [9].

Such characteristics were determined for a number of bypass turbofan engines distinguished substantially both in thrust and in bypass ratio $m$ (from 0.5,…,1.1 to 2.5,…,5.0), and for airframes of trunk-route aircrafts.

A well-known impedance testing technique was used: for the determination of these characteristics, the structures were excited by an electrodynamics shaker while the harmonic input force amplitude was constant and its frequency was varying automatically within the studied range.

Compliance values of sub-systems such as the engine and the airframe were determined by the method of test effect within the 10–500 Hz frequency range. The investigated system linearity was verified by changing the effective force by several times.

Analysis of obtained data makes it possible to divide the frequency range of investigation into three sub-ranges characterized by certain dynamic behaviors of the engine and consequently each of the said ranges can be provided with its special mathematical model—simple and clear enough (Fig. 5).

Modifications of frequency characteristics of the engine's dynamic compliances are presented in Fig. 5.

The straight line in double-log scale ($x$-axis—frequency, $y$-axis—compliance) with a slope factor of 12 dB per octave corresponds to the function $C(f) = 1/m(2\pi f)^2$, ($C(f)$—dynamic compliance), which is a feature of a rigid body.

The straight line parallel to the $x$-axis is a feature of an elastic element, whereas the one with the slope of 6 dB per octave belongs to an elastic–dissipative element.

Generalization of the performed investigations has revealed that the dynamic behavior of an advanced gas turbine engine body corresponds to the rigid-body model for frequencies below 20–40 Hz, depending on the bypass ratio.

If the bypass ratio is increased up to an estimated 8,…,12, it could be expected that the upper boundary of the rigid-body-like dynamic behavior of the engine does not exceed 10 Hz.

Within a wide range of rotor frequencies, the dynamic behavior of the engine body corresponds to the model of an elastic–inertial system or to an elastic–dissipative element. It differs substantially from the idealized rigid-body model of an aircraft gas turbine engine, both by the value of dynamic compliance module and by the type of dynamic behavior [10].

As is evident from presented data, the dynamic behavior of the airframe (at engine brackets attachment points) depends on the frequency range (Fig. 6). The elastic airframe's behavior, accepted in many calculation models, is limited by a rather narrow frequency range (50–100 Hz), which does not embrace the rotor frequency range of the many-shaft engine.

An example of vibroacoustical compliance transfer function between a point of impact (place of bracket attachment of engine) and a point in the cabin (place of noise monitoring) is presented in Fig. 7.

Transfer function characterizes the acoustic response of the cabin to the vibration impact of the engine. The points on the curve denote cruising rotation regimes for three engine types planned to be installed on the aircraft.

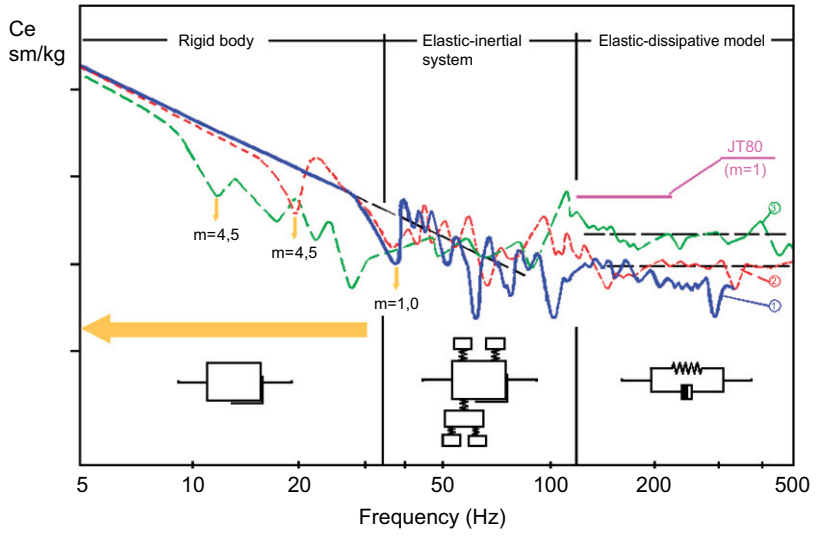


Fig. 5. Dynamic compliances of the engine body at attachment points, 1—$m = 1$; 2—$m = 2{,}5$; 3—$m = 4{,}5$.

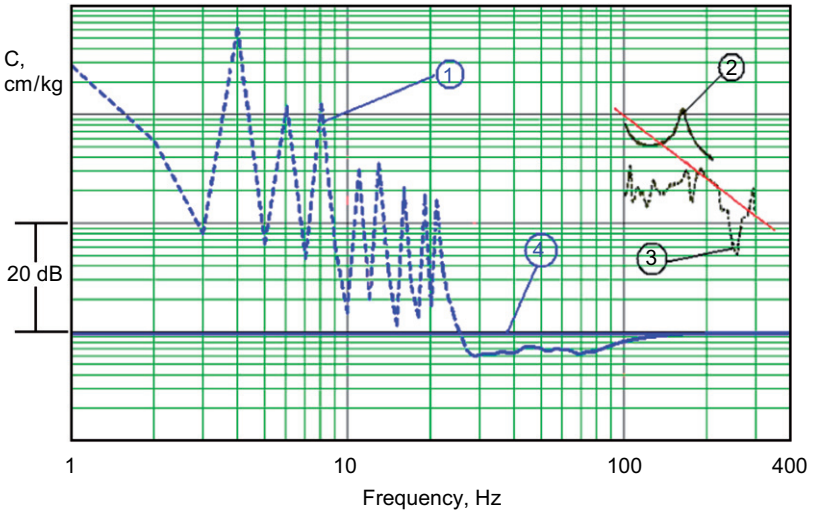


Fig. 6. The module compliance of the airframe. 1—Proposed numerical model for the airframe into account of experimental results; 2—real dynamic compliance of mount bracket for JT8D on DC-9; 3—real dynamic compliance of mount bracket for D30-KU on TU-154 M; and 4—model of airframe as elasticity.

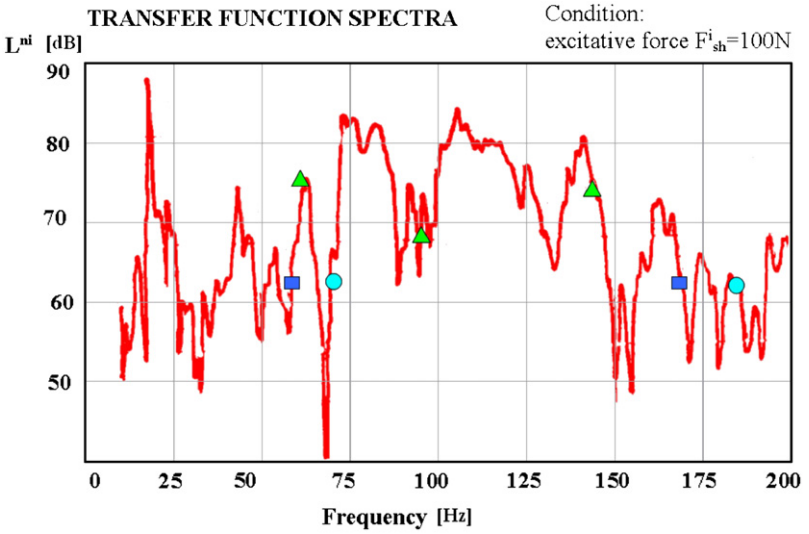


Fig. 7. Vibroacoustic conductivity (marked points-cruise modes for different engines).

It should be noted that at the same acoustic impact level, the difference of the response of the cabin reaches 15 dB for different engines at cruising regimes.

The obtained characteristics and algorithms described above have allowed us to calculate the expected noise due to vibration impact of the engine. Thus, high-level frequency components of noise generated by vibration impact from the power plant can be observed in the cockpit. The calculation data have been confirmed by the results of experimental measurement (Fig. 8).

The comparison of the expected noise and the experimental data yields both a good convergence of fan rotor harmonic level and a possibility of high-intensity low-frequency components generation at the operation level of engine vibration.

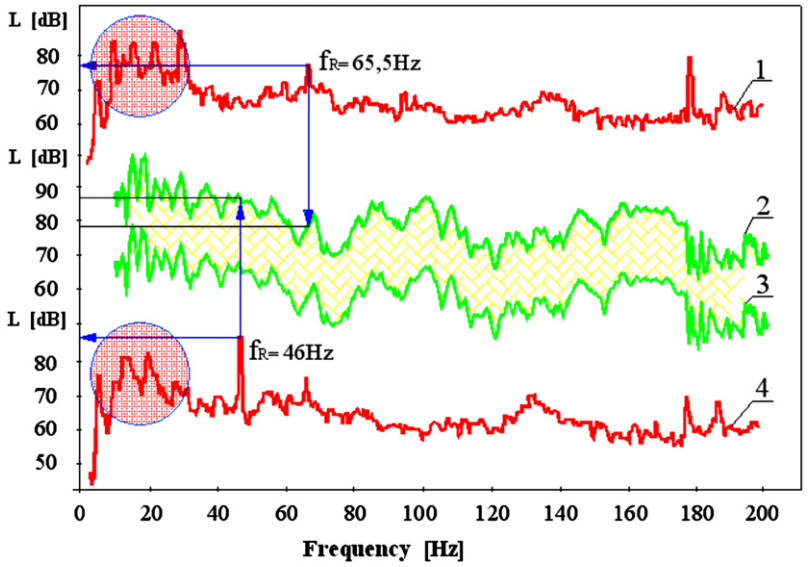


Fig. 8. Structure-borne sound in cabin. 1,4—experimental data, $V_E = 10\,\text{mm/s}$; and 2,3—prediction data, $V_E = 10\,\text{mm/s}$ and $V_E = 1\,\text{mm/s}$ correspondingly.

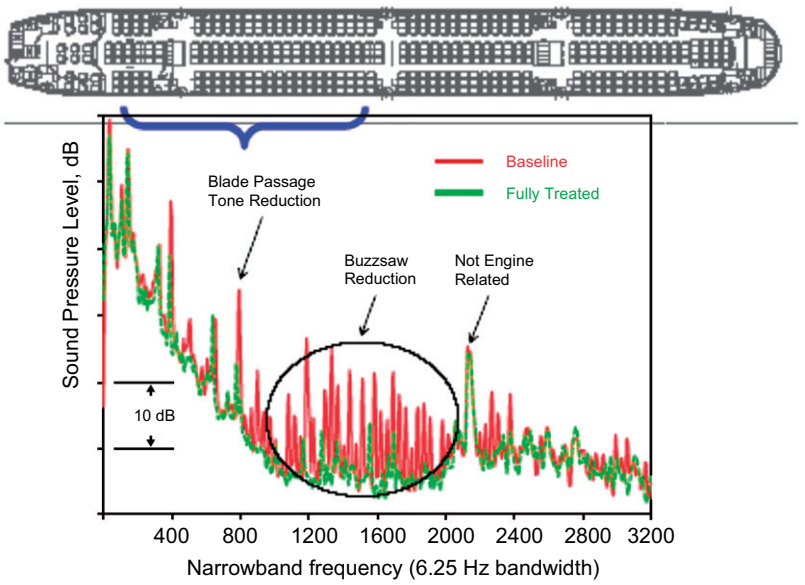


Fig. 9. Forward cabin interior noise reduction as a result of acoustic smooth inlet.

Carried out on aircraft-demonstrator QTD-2 (Boeing-777 with engine GE-90-115B with bypass ratio—8), modern investigations of new technologies for community noise decreasing have demonstrated decreasing community noise and internal noise in the cabin [11].

Noted progress of internal noise decreasing in the cabin are connected with actions on noise decreasing in the source (blades, chevrons) and with propagation paths (increase of sound-absorbing panels area at entry of inlet and increase its efficiency). This progress is due to external acoustical impact decreasing on fuselage facing the front part and the tail end of the cabin.

On decreasing of fan noise, the low-frequency discrete components will determine the acoustical climate in the cabin. It was confirmed by new investigations on the airframe QTD-2 (Fig. 9), where low-frequency components rise over 30–40 dB.

The approach based on the application of nonlinear elastic elements with quazi-zero elasticity is proposed for decreasing low-frequency impact.

The necessity of new vibroisolation mounting relates with: (1) the extension of the vibration spectrum of modern engines and its tendency to shift towards the low-frequency region; (2) insufficient efficiency of the existing vibration protection, developed on the basis of out-of-date computation models, especially in the low-frequency region; (3) change of dynamic characteristics of airframe and engine bodies at attachment points with the increase of engines' bypass ratio.

## 4. Vibroisolation model and investigations

Necessary vibroprotection level can be supplied by vibroisolation blocks with nonlinear elastic characteristics with a quasi-zero stiffness work field for the calculated force (for example, at cruise).

Such a device provides a large static elasticity of vibroisolation mounting and can function in a wide range of dynamical forces and narrow displacement range.

All these requirements are satisfied using a vibroisolation mounting based on initially deformed elements with a quasi-zero stiffness zone. It contains quasi-unstable elements of different configurations with special nonidealities of shape and boundary conditions determining elastic characteristic: soft nonlinear with a quasi-zero work field at the calculated force [8].

The mounting functioning principle is based on using of small elasticityies of such elements near their field of stability loss from static forces in attachment knots at calculated regimes. In Fig. 10, the elastic characteristic of element mount (a), the oriented mount on different static loads (b) and the example mount strut (c) are presented.

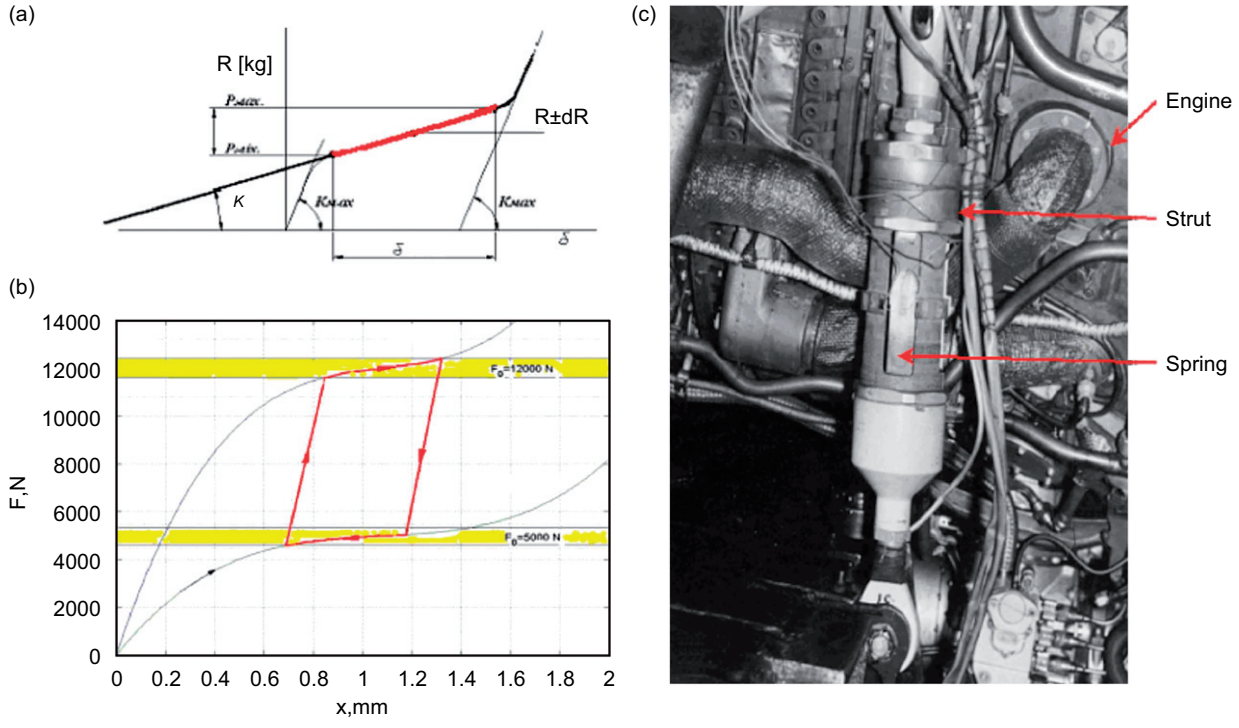


Fig. 10. Elastic characteristic of an element mount (a); oriented mount on different static loads (b); and example mount strut (c).

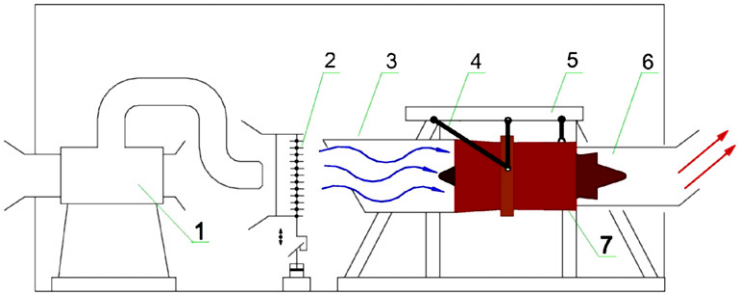


Fig. 11. Test engine bench. 1—Air injection system; 2—vibrating system; 3—air inlet unit; 4—mounting struts; 5—engine base frame; 6—exhaust unit; and 7—engine.

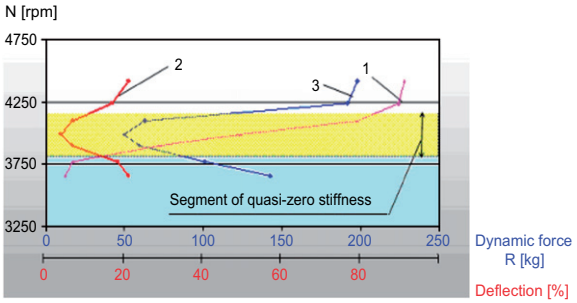


Fig. 12. Experimental testing of a new vibroisolation device. 1—Elastic characteristic; 2—rotor component; and 3—low-frequency component.

The computational investigations of low-frequency vibroisolation mounting dynamic model were carried out. Numerical investigations allowed one to obtain a significant decrease of oscillation amplitude in case of nonlinear elastic characteristics using all the external dynamical force types [12]. Numerical data are in qualitative and quantitative accordance with experimental data.

Proposed mounting has been investigated on a special rig (Fig. 11), including a gasturbine engine and unit, creating low-frequency forces from the engine. Results of suspension tests showed that the engine with such suspension oscillation's own frequencies exceed 3.5 Hz at a static displacement of 2.5 mm. Dynamic force passed via suspension from the engine decreased by 12–14 dB at frequencies 8–60 Hz (Fig. 12).

## 5. Conclusions

We suggested a method of structural noise calculation, which takes into account real dynamic characteristics, such as the dynamic compliance of the engine body and the airframe. Selecting power plants for airplanes of the new generation, besides solving problems of community noise, should also include developing a high-performance system of vibroprotection of crew and passengers for the maintenance of comfortable conditions and flight safety.

## References

[1] B.N. Shivashankara, Recent advances in aircraft noise reduction and future technology needs, *International Symposium: With technologies for future aircraft noise reduction?* Arcachon, France, 2002.

[2] V.S. Baklanov, A.V. Zayakin, E.A. Orlenko, S.S. Postnov, Expected viroacoustical spectrum of high bypass ratio power plant, *Conference on Condition Monitoring*, Cambridge, 2005.

[3] M. Alves-Pereira, M.S. Castelo Branko, J. Motylewski, A. Pedrosa, N. Castelo Branko, Airflow-induced infrasound in commercial aircraft, *INTER-NOISE 2001*, The Hague, The Netherlands, August 2001.

[4] S. Rubin, F.A. Biehl, Mechanical impedance approach to engine vibration transmission into an aircraft fuselage, *Aeronautic and Space Engineering and Manufacturing Meeting*, SAE, Paper No. 670873, 1967.
[5] V.S. Baklanov, V.M. Vul, Vibration isolation of aviation power plants taking into account real dynamic characteristics of engine and aircraft, *Proceedings of the Second International Congress on Recent Developments in Air- and Structure-Borne Sound and Vibration*, Vol. l, March 4–6, 1992, Auburn University, USA.
[6] J.F. Unruh, Procedure for evaluation of engine isolators for reduced structure-borne noise transmission, *Journal of Aircraft* 20 (1) (1983).
[7] V. Baklanov, A. Zayakin, E. Orlenko, S. Postnov, The calculation of structural noise in cabin for aircraft with high-by-pass ratio engines, *Proceedings of the 11th AIAA/CEAS Aeroacoustics Conference*, Monterey, CA, May 23–25 2005, AIAA 2005–3034.
[8] V.S. Baklanov, I.V. Golov, S.S. Postnov, Vibroisolation of power plants for new generation airplanes with engines of high by-pass ratio, *Proceedings of the 10th AIAA/CEAS Aeroacoustics Conference*, Manchester, UK, 10–12 May 2004, AIAA 2004–2823.
[9] V.S. Baklanov, Dynamic model of engine-mount-airframe system of trunk-aircraft basing on results of impedance data tests at attachment points, *Ninth International Congress on Sound and Vibration*, July 2002, Orlando, FL, USA.
[10] V.S. Baklanov, S.L. Denisov, Numerical simulation of the system "engine-mounting-airframe" according to experimental data results, *Proceedings of the 12th AIAA/CEAS Aeroacoustics Conference (27th AIAA Aeroacoustics Conference)*, Cambridge, MA, May 8–10, 2006, AIAA-2006–2663.
[11] E. Nesbitt, Jia Yu, et al., Quiet technology demonstrator 2 intake liner design and validation, *12th AIAA/CEAS Aeroacoustic Conference,* Cambridge, MA, 8–10 May 2006.
[12] V. Baklanov, S. Postnov, A. Zayakin, The computational investigation of low-frequency vibroisolation mounting dynamic model, *Proceedings of the 12th AIAA/CEAS Aeroacoustics Conference (27th AIAA Aeroacoustics Conference)*, Cambridge, MA, May 8–10, 2006, AIAA-2006–2658.